Ab Initio Study of Hydrogen-Bond Formation between Cyclic Ethers and Selected Amino Acid Side Chains

Peter I. Nagy* and Paul W. Erhardt

Center for Drug Design and Development, College of Pharmacy, The University of Toledo, Toledo, Ohio 43606-3390

Received: February 21, 2006; In Final Form: October 11, 2006

Binding energies for hydrogen-bonded complexes of six cyclic ethers with five hydrogen-bond donor molecules that mimic selected amino acid side chains have been calculated at the MP2/6-31G*, MP2/6-31+G*, MP2/6-311++G**(single point), and MP2/aug-cc-pvtz levels, using geometries obtained with or without counterpoise corrections throughout the geometry optimization. The calculated basis set superposition error (BSSE) amounts to 10−20% and 5−10% of the uncorrected binding energies for the neutral and ionic species, respectively, at the MP2/aug-cc-pvtz level. The authors conclude that the O···H distances in the hydrogen bonds and binding energies for the studied systems may be determined with uncertainties of up to 0.08 Å and 1−2 kcal/mol, respectively, in comparison with the MP2/aug-cc-pvtz values at a reasonable computational cost by performing standard geometry optimization at the MP2/6-31+G* level. Hydrogen-bond formation energies are more negative for cyclic ethers compared to their counterparts with a C═C double bond in the ring next to the oxygen atom. The less negative hydrogen-bonding energy and the increased O···H separation have been attributed to the reduced basicity of the ether oxygen when the lone pairs can enter conjugation with the π-electrons of the C_α═C_β double bond. The present study is the first step toward the development of an affordable computational level for estimating the binding energies of natural product, fused ring ether systems to the human estrogen receptor.

Introduction

Hydrogen-bond formation is a commonly observed intermolecular interaction between polar molecules that occurs, as one of its important biochemical manifestations, during reversible ligand binding by protein receptors. Numerous studies have been directed toward understanding such events.[1] Cationic (protonated lysine, arginine, and histidine) and anionic (aspartate, glutamate) amino acid side chains can behave as proton donors and acceptors, respectively. Neutral polar side chains such as serine, threonine, cystein, and histidine can act as both proton donors and acceptors. The backbone peptide bond can also play an important role in hydrogen-bond formation either with amino acid side chains or with complementary sites on the ligand.

For ligands, aliphatic and aromatic amines, alcohols, carboxylic acids, C═O, −SH, $-SO_2$, −CN, and even halogens, can all serve as sites for protein−ligand hydrogen bonds. While many of these can form strong hydrogen bonds with the amino acid side chains, the strongest forms are observed for the groups that can be ionized during the interaction, such as carboxylate anions or ammonium and guanidinium cations.

Considerably less is known about the hydrogen bonds formed with ethers.[2] Intermolecular hydrogen bonds have been studied between crown ethers and a hydronium ion as well as with neutral polar molecules;[3a−d] a water molecule and a model compound for poly(vinyl-methyl ether);[3e] complexes of dimethylether with nitric acid,[3f,g] haloforms,[3h] and methanol;[3i] diethyl ether and aniline;[3j] and for the multiply hydrated 2-phenoxyethanol.[3k] In an intramolecular setting, hydrogen bonding to an ether oxygen has been studied in an amide−ether system,[4a] for methyl-[4b] and vinyl[4c] ethers of ethylene glycol, and for the β-O-4 linkage of lignin.[4d] No consistent study appears to have been undertaken for cyclic ethers, despite this system's importance in substances such as the saccharides, and in complicated fused ring systems such as the glyceollin natural products.

The glyceollins, as found in soybean, are pentacyclic systems that contain both alcoholic OH groups and an ether ring. Simple molecular mechanics geometry optimization suggests that these molecules can be superimposed with the human hormone 17β-estradiol (E2), which is a known agonist for the human estrogen receptor (hER).[5] The geometric fit and the nearly overlapping positions for the ether and alcoholic oxygens in the two molecules raise the possibility that the glyceollins may have estrogen activity. Indeed, there is increasing evidence that some natural and nonnatural chemicals have the potential to modulate the human endocrine system by mimicking endogenous hormones such as the androgens and estrogens.[6]

That the glyceollins may reach the hER and preferentially interact with its different subtypes presents an intriguing possibility and is of potential interest in our laboratories. To investigate this situation by taking a computational approach, geometric parameters and hydrogen-bond formation energies have been calculated in the present study at the MP2 level with different basis sets for a series of cyclic ethers with small, polar molecules representing various amino acid side chains. Comparison of the MP2/6-31G*, MP2/6-31+G*, MP2/6-311++G**, and MP2/aug-cc-pvtz results for the studied systems allows for assessment of the basis set effect on both the optimized geometry and the binding (or hydrogen-bond formation) energy.

* Author to whom correspondence should be addressed. E-mail: pnagy@utnet.utoledo.edu.

10.1021/jp061113t CCC: $33.50
Published on Web 12/05/2006

SCHEME 1: Cyclic Ethers Studied: OCBe (Oxocyclobutene), DHF (Dihydrofuran), OCHD (Oxocyclohexa-2,4-diene), OCB (Oxocyclobutane), THF (Tetrahydrofuran), and OCHe (Oxocyclohex-3-ene)

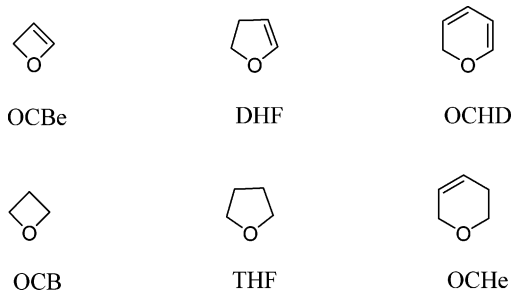

Methods and Calculations

Hydrogen bonds for six cyclic ethers (Scheme 1) have been studied across five donor amino acid side chain mimics: (1) CH_3OH (mimic for serine and threonine), (2 and 3) neutral and protonated imidazole (mimics for histidine), (4) $CH_3NH_3^+$ (mimic for protonated lysine), and (5) methyl-guanidium cation (mimic for protonated arginine). All studies were performed at the ab initio MP2 level.[7,8] Geometry optimizations for 6×5 hydrogen-bonded pairs were performed by applying the 6-31G*, 6-31+G*,[7] and aug-cc-pvtz basis sets[9] (Figures 1−5). Local energy-minimum characters were certified by frequency analysis at the non-CP MP2/6-31G* and MP2/6-31+G* levels as well as at the CP/MP2/6-31G* level. (CP and non-CP optimizations refer to geometry optimizations with and without considering the basis set superposition error (BSSE) term, respectively, throughout the process, see below.) Thermal corrections (applied for the water dimer) for free energies utilized the rigid rotor-harmonic oscillator approximation.[10]

A recurring problem in the binding energy analysis and structure determination of van der Waals complexes is the role of the basis set superposition error, BSSE.[11] The classical correction procedure for this error is the Boys−Bernardi method.[12] Instead of calculating the ΔE^{uncor}, uncorrected binding energy as

$$\Delta E^{uncor} = E(\text{complex}) - E(\text{A})^m - E(\text{B})^m \qquad (1)$$

where E(complex) stands for the energy of the hydrogen-bonded complex (an ether−amino acid mimic system in the present case), and $E(\text{A})^m$ and $E(\text{B})^m$ stand for the energies of the isolated component molecules A and B in the monomer basis set (superscript m); the Boys−Bernardi method considers the so-called counterpoise binding energy, ΔE^{CP}, as

$$\Delta E^{CP} = E(\text{complex}) - E(\text{A})^d - E(\text{B})^d \qquad (2)$$

Superscript d refers to the dimer basis set. In the original version of this method, the geometries of the elements of the complex were considered in their separately optimized forms even throughout the formation of the complex. To minimize the total energy of the complex, the geometries of the elements undergo some changes, leading to a necessary energy increase in their energy.[13]

Definition of the BSSE may slightly differ by different authors.[11,14] In a seven-point calculation for a complex, Nagy et al.,[15] providing explicit formulas for the terms, defined the BSSE devoid of the geometry distortion energy for the components, GEOM.

$$\Delta E^{cor} \equiv \Delta E^{uncor} - \text{BSSE} = \Delta E^{CP} + \text{GEOM} \qquad (3)$$

GEOM is always a positive energy term in eq 3, whereas BSSE is of negative sign because the larger basis set used in calculations for the complex allows a more adequate description of the electron distribution for each component of the hydrogen-bonded system, and the resulting energy lowers. ΔE^{CP} is the counterpoise corrected hydrogen-bond formation energy as calculated at geometries for the elements optimized in the complex. ΔE^{cor} differs from ΔE^{CP} by the geometry distortion energy of GEOM.

Whereas it is generally accepted that the BSSE causes a nonphysical stabilization for the calculated interaction energy, ΔE^{uncor}, the correct method for its estimation is not clear. ΔE^{uncor} obviously depends on the calculated equilibrium geometry for the complex. The following question may be raised: does BSSE affect only the energy results, or does it also affect the calculated optimal complex geometry, mainly the equilibrium distance for the H-bond?

Simon et al.[14] performed geometry optimizations for small hydrogen-bonded complexes where the BSSE was considered in every step of the optimization (referred to hereafter as counterpoise-corrected, CP-optimization). A modified interaction-energy expression was applied and the stationary point was sought for this term. This method is now available in Gaussian 03,[16] and it was applied in parallel with the standard gradient optimization during our studies.

In the standard method (hereafter referred to as a non-CP corrected optimization), the minimum energy for the dimer structure is reached, whereas the CP optimization finds a structure providing a minimum for the E(complex) − BSSE expression. Comparing non-CP and CP energy terms, the following inequalities hold for the optimized structures:

$$E(\text{complex, CP}) - \text{BSSE(CP)} \le E(\text{complex, non-CP}) - \text{BSSE(non-CP)} \qquad (4a)$$

$$E(\text{complex, non-CP}) \le E(\text{complex, CP}) \qquad (4b)$$

From eqs 1, 4a, and 4b then, it follows that ΔE^{uncor} (non-CP) $\le \Delta E^{uncor}$ (CP), ΔE^{cor} (CP) $\le \Delta E^{cor}$(non-CP), and BSSE(non-CP) $\le$ BSSE(CP). Both ΔE^{uncor} and BSSE are of negative values, and $\Delta E^{cor} = E(\text{complex}) - E(\text{A})^m - E(\text{B})^m - \text{BSSE}$. Whereas the inequalities regarding the uncorrected and corrected binding energies are trivial consequences of their definitions upon the optimization method, the inequality with respect to the BSSE values tells that the calculated BSSE must be more negative with the non-CP compared to the CP optimization.

The inequalities above are valid in case of a given basis set used in the calculations but state nothing about the convergence of the ΔE values. When the basis set increases, the molecular energies for the optimized complex and the components decrease monotonically. The ΔE^{uncor} values are calculated, however, as differences of the corresponding members of two monotonically decreasing sets, and the differences need not change monotonically. Because of the latter, we obtained both increases and decreases in ΔE^{uncor} upon the basis set extension (Tables 2 and 3). Accordingly, no monotonic change for $\Delta E^{cor} = \Delta E^{uncor} -$ BSSE is necessary even if BSSE decreases (in absolute value) monotonically (Table 1, S1).

The effects of the two types of geometry optimizations on the structure and binding energies of the complexes have been compared here at the MP2/6-31G* and MP2/6-31+G* levels and upon calculations up to the MP2/aug-cc-pvtz level for three selected systems: the water dimer, for which experimental data are available, and for the oxocyclobutane···CH_3OH and the oxocyclobutane···$CH_3NH_3^+$ systems, which were considered as

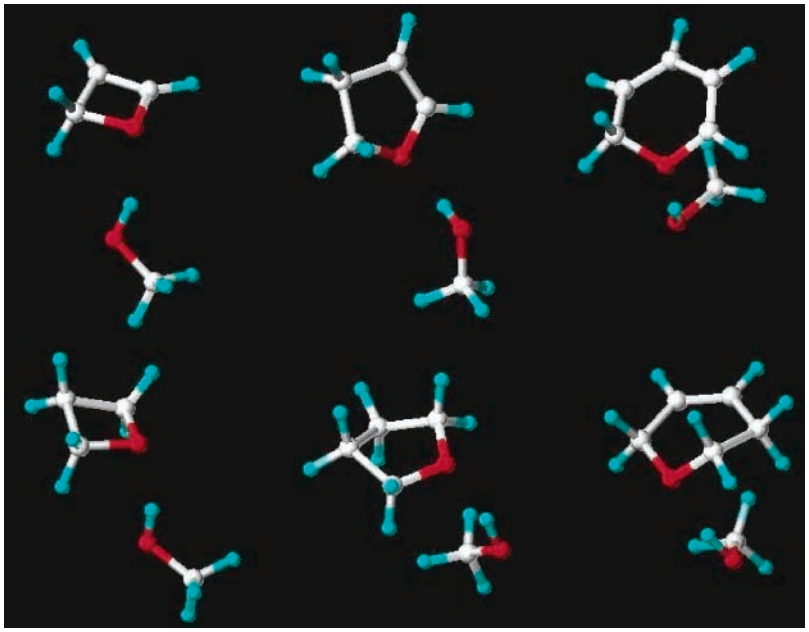

Figure 1. MP2/aug-ccpvtz optimized complexes of cyclic ethers with CH_3OH. Color code: C, white; H, cyan; O, red; N, blue. Ethers from left to right, upper row: oxocyclobutene, dihydrofuran, oxocyclohexadiene-2,4; lower row: oxocyclobutane, tetrahydrofuran, oxocyclohexene-3.

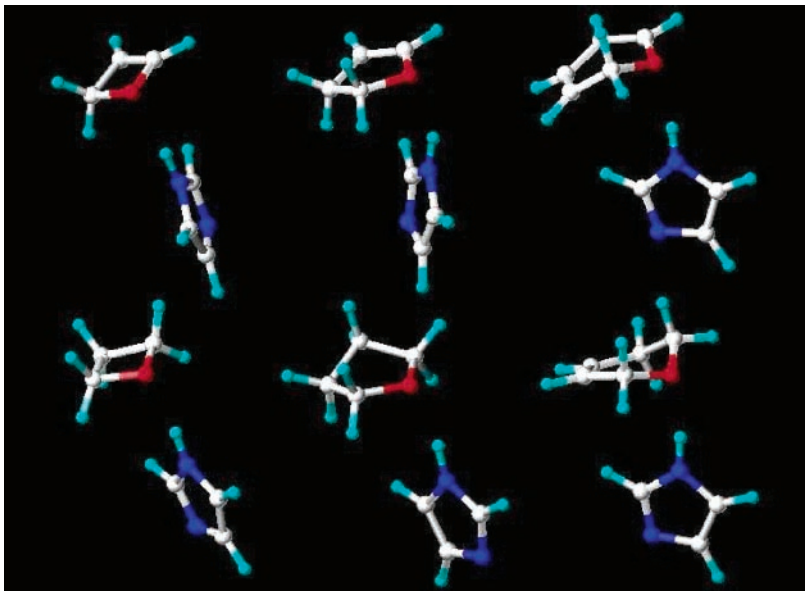

Figure 2. MP2/aug-ccpvtz optimized complexes of cyclic ethers with the neutral imidazole. For the color code and the ether components, see Figure 1.

prototypes for the neutral and ionic hydrogen-bonded cyclic ethers, respectively.

Results and Discussion

Water Dimer. With a large basis set in high-level calculations, CP and non-CP optimizations have to provide identical results since the BSSE converges to zero, and thus the optimized structures must be identical. A goal in the present study was to explore how fast convergence can be achieved when relatively small basis sets are applied. This problem is important from a practical point of view because only relatively small basis sets are affordable even for model systems of biologically interesting molecules in general.

It was pointed out by Simon et al.[14] that the CP geometry optimization leads to larger heavy atom separation in the X−H···Y bond than the standard procedure. These authors performed calculations at the HF and MP2 levels, using the 6-31G(d,p) and the D95 ++(d,p) basis sets. The calculated BSSE values amounted to 25−30% of the ΔE^{uncor} binding energy from the non-CP optimization. It is reasonable to assume that such a large overstabilization influences not only the binding energy but the obtained equilibrium geometry as well.

Hobza and Havlas[17] have argued in favor of the CP optimization because they determined that the non-CP optimization fails to find a stationary point for the quasi-linear structure of the HF dimer, in contrast to the CP optimization, at the MP2/6-31G** level. This is a serious warning that non-CP optimization may lead to incorrect geometry with a small basis set. Upon increasing the basis set to the MP2/6-311G(2d,p) level, however, they found both the cyclic and the quasi-linear geometries either with the non-CP and CP optimization.

In contrast, the need for the CP optimization has been questioned by other authors. In a series of high-level calculations for the water dimer, Halkier et al.[18] noticed a rapid convergence

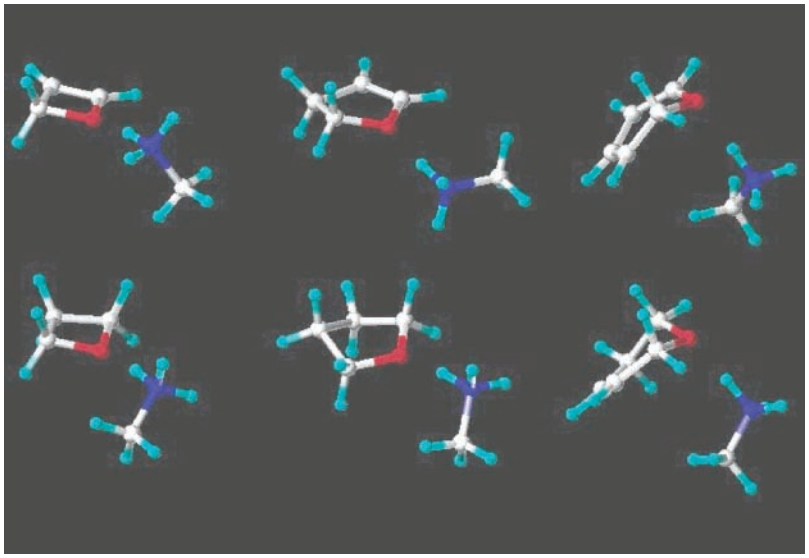

Figure 3. MP2/aug-ccpvtz optimized complexes of cyclic ethers with $CH_3NH_3^+$. For the color code and the ether components, see Figure 1.

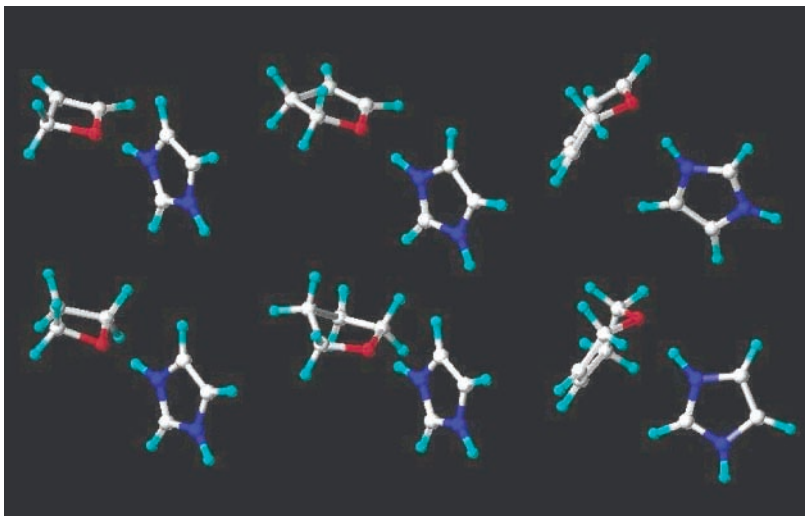

Figure 4. MP2/aug-ccpvtz optimized complexes of cyclic ethers with the protonated imidazole. For the color code and the ether components, see Figure 1.

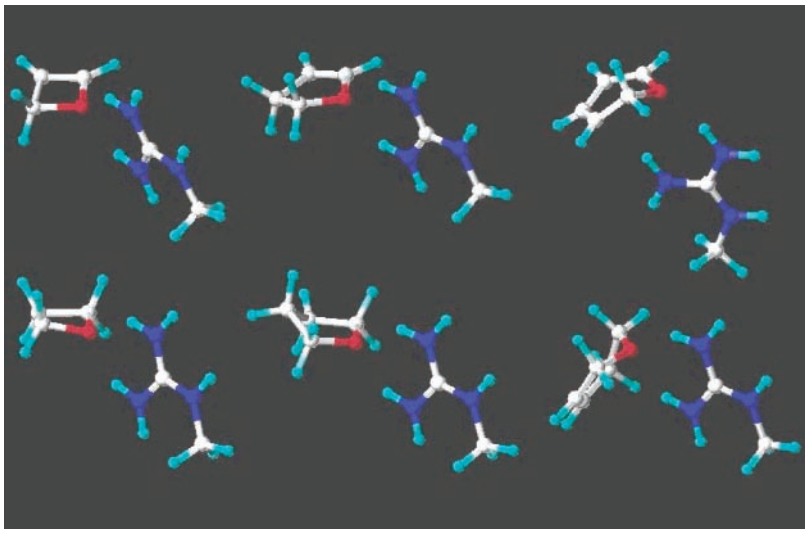

Figure 5. MP2/aug-ccpvtz optimized complexes of cyclic ethers with the guanidinium cation. For the color code and the ether components, see Figure 1.

of the MP2/CP optimized O···O equilibrium separation to the MP2/non-CP optimized value with basis sets aug-cc-pvXz, X= D,T,Q. With large basis sets, the BSSE becomes small. Thus, the non-CP optimization is useful when a satisfactorily large basis set has been applied. But what then constitutes a satisfactorily large basis set?

TABLE 1: Ab Initio MP2 Results for the Water Dimer with C_s Symmetry[a]

	O···O	O···H	O−H···O	$X_aO_aO_d$	$O_aO_dX_d$	ΔE^{uncor}	BSSE	ΔE^{cor}
			Non-CP Optimization					
6-31G*	2.914	1.958	166.1	78.9	−61.4	−7.32	−2.24	−5.08
6-31+G*	2.905	1.930	174.5	51.0	−56.6	−7.01	−2.07	−4.94
6-311++G**	2.916	1.951	178.5	41.9	−52.7	−6.07	−1.63	−4.45
aug-cc-pvtz								
C_s	2.909	1.947	171.6	56.2	−57.9	−5.18	−0.47	−4.71
C_1	2.907	1.945	171.7	56.6	−57.8	−5.18	−0.47	−4.71
			CP Optimization					
6-31G*	2.976	2.003	175.7	52.8	−54.8	−7.07	−1.70	−5.37
6-31+G*	3.011	2.040	172.2	52.6	−58.0	−6.84	−1.76	−5.08
6-311++G**	3.021	2.058	176.2	42.0	−54.4	−5.95	−1.39	−4.56
aug-cc-pvtz	2.932	1.971	171.3	54.4	−58.1	−5.17	−0.45	−4.72
expt[b]	2.976(+0.000, −0.030)			57(5)	−51(10)			

[a] Distances in Å, angles in degree, energies in kcal/mol. Subscripts "a" and "d" stand for the acceptor and the donor molecule, respectively. X is a dummy atom along the corresponding HOH bisector, and the XOO angles were calculated in accord with the definition of υ_a and υ_d in ref 19. $\Delta E^{cor} = \Delta E^{uncor} - BSSE$. [b] Reference 19.

Using the non-CP MP2 geometry optimization for the water dimer (Table 1), the calculated equilibrium O···O distance is in the narrow range of 2.905−2.916 Å despite the large difference in the basis sets increasing from 6-31G* to aug-cc-pvtz. The experimental value is 2.946−2.976 Å.[19] The $X_aO_aO_d$ and $O_aO_dX_d$ angles (for the letter codes, see the footnote in Table 1), however, change remarkably with the increasing basis set. With the 6-31+G* and aug-cc-pvtz sets, the calculated values are within or close to the experimental limits. The $X_aO_aO_d$ value was calculated too large and too small with the 6-31G* and 6-311++G** basis sets, respectively. In the interpretation of the experimental results for the water dimer, Odutole and Dyke[19] assumed a C_{2v} symmetry for the hydrogen acceptor water. Symmetry unrestricted geometry optimizations with small basis sets led to geometries far from the nearly C_s experimental structure. For useful comparison of the calculated and experimental results, C_s symmetry-restricted optimizations were performed in all cases, whereas an unrestricted optimization with the aug-cc-pvtz basis set was also performed. In the latter calculation, the intermolecular geometric parameters slightly changed and the C_s symmetry was destroyed by torsion angles of $H_dO_dH_d\cdots O_a = 179.92°$ and $H_aO_a\cdots H_dO_d = (+58.09; -57.91)$, but the C_1 geometry was more stable than the C_s geometry by only 2×10^{-7} au, and the calculated binding energies and free energies are stable within 0.01 kcal/mol (Tables 1 and 2).

The uncorrected binding energy, ΔE^{uncor}, becomes monotonically less negative with the increasing basis set, in parallel with the monotonic decrease in the absolute value for BSSE. Although both terms change monotonically, their difference, $\Delta E^{cor} = \Delta E^{uncor} - BSSE$, need not also change monotonically, as mentioned above. Indeed, the ΔE^{cor} value was calculated at −4.94, −4.45, and −4.71 kcal/mol, using the 6-31+G*, 6-311++G**, and aug-cc-pvtz basis sets, respectively, throughout the geometry optimizations. The most conspicuous consequence of the CP optimization is the remarkably increased equilibrium O···O distance. The obtained value of 2.976 Å at the MP2/6-31G* level coincides with the upper limit of the experimental value. Considerably larger values 3.01−3.02 Å were obtained with the 6-31+G* and 6-311++G** basis sets when the MP2/CP optimization was applied. A value close to the lower experimental limit was obtained when the aug-cc-pvtz basis set was used.

Halkier et al.[18] obtained equilibrium O···O separation of 2.895 Å both at the CCSD(T)/aug-cc-pvtz and the MP2/aug-cc-pvqz levels with non-CP optimization and estimated that the correct O···O value in the water dimer should be about 2.90 Å in contrast to the experimental value of 2.946−2.976 Å. However, such a large basis set cannot be used routinely for larger systems, for example, for simple hydrogen-bonded ethers, and even less so for hydrogen bonds between ethers consisting of fused rings and simple amino acid side chain mimics such as methylguanidine. Thus, the problem remains whether CP optimization is to be used with relatively small basis sets for obtaining reliable geometry for such complexes. The non-CP optimization provided optimal O···O values very close to each other with the four basis sets in Table 1, but the $X_aO_aO_d$ and $O_aO_dX_d$ angles were overestimated at the MP2/6-31G* level. The calculated geometric parameters and the ΔE^{cor} values are, however, close at the MP2/6-31+G* and the MP2/aug-cc-pvtz levels. Taken together, the similar values suggest that the MP2/6-31+G* optimization level may be a useful compromise between precision and affordable computational cost.

Curtiss et al.[20] found an enthalpy change of -3.59 ± 0.5 kcal/mol at $T = 373$ K for the water dimerization process on the basis of thermal conductivity measurements. The corresponding dimerization energy is -5.44 ± 0.7 kcal/mol. From theoretical studies, Halkier et al. concluded that $\Delta E = -5.0 \pm 0.1$ kcal/mol.[18] Finally, Curtiss et al.[20] found that the equilibrium constant is 0.0111 atm^{-1} for the $2H_2O \leftrightarrow (H_2O)_2$ dimerization reaction at $T = 373$ K, which corresponds to free-energy change of $\Delta G = 3.34$ kcal/mol.

Table 2 summarizes our energy and free-energy results for the water dimerization. Where the temperature is not explicitly indicated, the upper and lower sets were calculated at $T = 298$ and 373 K, respectively. The ΔE^{cor} values are at the upper end of the experimentally derived and the Halkier et al. reported values. Except for the 6-31G* basis set, this term shows weak dependence on the applied basis set. Thus, an important conclusion may be drawn: CP and non-CP optimizations could lead to remarkably different geometries, but the corresponding BSSE-corrected interaction energies change only a little for the water dimer. The ΔZPE terms show deviations up to 0.4 kcal/mol, depending on the applied basis set within an optimization series. In contrast to the ΔE^{cor} values, however, the ΔZPEs calculated with the 6-31+G* as well as the 6-311++G** basis sets differ considerably from the CP and non-CP optimizations. The corresponding equilibrium OO distances also differ largely, by about 0.1 Å, and this structural departure is reflected in the remarkable deviations of the ΔZPE values obtained with the two optimization methods.

The calculated thermal vibrational correction $\Delta(H_{vibr}(T) - ZPE)$ is nearly equal with any basis set and increases by about 0.8 kcal/mol between $T = 298$ and 373 K. The increase of the

TABLE 2: Calculated Thermodynamic Parameters for the Water Dimerization at $T = 298.15$ and 373 K and at $p = 1$ atm Using Different Basis Sets at the ab Initio MP2 Level[a]

	ΔE^{cor}	ΔZPE	$\Delta(H_{vibr}(T) - \text{ZPE})$	$\Delta H(T)$	$-T\Delta S(T)$	$\Delta G(T)$
Non-CP Optimization						
6-31G*	−5.08	2.30	1.86	−3.29	6.89	3.60
			2.62	−3.12	8.43	5.31
6-31+G*	−4.94	2.52	1.74	−3.05	6.56	3.51
			2.49	−2.89	8.03	5.14
6-311++G**	−4.45	2.37	1.81	−2.64	7.18	4.54
			2.57	−2.47	8.79	6.32
aug-cc-pvtz						
C_s, $T = 298$ K	−4.71	2.10	1.92	−3.06	6.03	2.97
C_1, $T = 298$ K	−4.71	2.10	1.91	−3.07	6.04	2.97
C_s, $T = 373$ K			2.70	−2.87	7.34	4.47
CP Optimization						
6-31G*	−5.37	2.28	1.87	−3.59	6.99	3.40
			2.64	−3.41	8.55	5.14
6-31+G*	−5.08	2.03	2.00	−3.42	5.72	2.30
6-311++G**	−4.56	1.91	2.07	−2.95	6.36	3.41
aug-cc-pvtz	−4.72	2.02	1.96	−3.11	5.91	2.80

[a] Energies in kcal/mol. $\Delta H = \Delta E^{cor} + \Delta\text{ZPE} + \Delta(H_{vibr} - \text{ZPE}) - 4RT$, $\Delta G = \Delta H - T\Delta S$. Where the temperature is not indicated regarding the C_s geometry obtained through the non-CP optimization, $T = 298.15$ and 373 K for the upper and the lower set, respectively. $4RT = 2.37$ and 2.96 kcal/mol at the two temperatures. Values referring to the CP optimized C_s geometries were calculated at $T = 298.15$ K.

$-T\Delta S(T)$ term is also nearly constant, 1.3−1.6 kcal/mol upon the elevation of the temperature, but the calculated $-T\Delta S(T)$ values at $T = 298$ K differ by more than 1 kcal/mol with different basis sets at the non-CP optimization level. This difference is basically due to the vibrational entropy term, because the rotational entropy, calculated in the rigid rotor approximation,[10] differed by only a few hundredths of a kcal/mol.

Comparing these terms with those reported by Curtis et al.[20] (ΔH and $-T\Delta S$ are −3.59 and 6.93 kcal/mol, respectively, at $T = 373$ K), our values are too positive such that the derived free-energy change, $\Delta G = \Delta H - T\Delta S$, is also higher than the experimentally derived value of 3.34 kcal/mol. The deviation in ΔG of at least 1.13 kcal/mol has been mainly attributed to the harmonic oscillator approximation, since the ΔE values deviate from the Halkier limit only by 0.1 and 0.3 kcal/mol with the basis sets 6-31+G* and aug-cc-pvtz, respectively.

Non-CP and CP Optimizations for Small Complexes of Oxocylobutane. Table 3 summarizes the structural and energetic changes for the $CH_3OH\cdots OCB$ and $CH_3NH_3^+\cdots OCB$ complexes (OCB = oxocyclobutane) as a function of the optimization method and the size of the basis set. For the major hydrogen-bond parameter, the O···H distance was calculated to be 0.03−0.10 Å and 0.01−0.06 Å longer for the $CH_3OH\cdots OCB$ and $CH_3NH_3^+\cdots OCB$ complexes when the CP instead of the non-CP optimization procedure was used. This finding is in line with our results for the water dimer above.

The larger basis set leads to smaller separation for the $CH_3OH\cdots OCB$ complex with both methods. In case of the water dimer, the change of the O···H distance was within a range of 0.01 Å when the non-CP optimization was used. Using this procedure for the methanol-oxocyclobutane ether complex in Table 3, the H-bond becomes shorter by 0.05 Å. By the CP optimization, the O···H separation was calculated at 1.93−1.94 Å with the first three basis sets and was shortened to 1.853 Å only at the MP2/aug-cc-pvtz level. The O···H separation for the $CH_3NH_3^+\cdots OCB$ pair does not change monotonically with the increasing basis set in either optimization method but shows convergence with the aug-cc-pvtz basis set.

The optimal X−H···O angle converges more slowly with increasing basis sets for the neutral compared to the ionic complex. Nonetheless, the 6-311++G** and aug-cc-pvtz optimized X−H···O angles are fairly close to each other for both complexes with either optimization method. Overall, the results indicate that the CP versus non-CP optimization, as well as the applied basis set, has large effects on the intermolecular hydrogen-bond geometric parameters.

The effect of the optimization method on the geometry of the elements of the complex may be implicitly assessed by considering the GEOM terms. These terms are up to 0.2 kcal/mol for the neutral $CH_3OH\cdots OCB$ system, which suggest only small geometry distortions for the CH_3OH and OCB molecules upon hydrogen-bond formation. The CP values are smaller than the non-CP GEOM energies, in accord with the calculated larger equilibrium O···H separations. This latter should lead to smaller geometric distortion for the individual molecules.

The GEOM term is, however, generally larger than 1 kcal/mol for the $CH_3NH_3^+\cdots OCB$ pair. This complex was considered as a prototype for the ionic hydrogen bond formed to a neutral cyclic ether. The remarkable intramolecular geometric distortion energy is independent of the optimization method and is attributed to the considerable elongation of the N−H bond involved in the N−H···O hydrogen bond. The N−H bond in the complex, $N-H_{comp}$, is stretched by 0.035−0.048 Å when compared to its value in the optimized monomer ($N-H_{mon}$). This large increase of bond length was found with all basis sets. Thus, the stretched N−H is not a consequence of the optimization method or the size of the basis set. For maximizing the interaction with the hydrogen-bond acceptor, the ionic proton donor partner undergoes remarkable geometry changes, which, however, entail a considerable increase of the internal energy of the given component. The equilibrium structure reflects the optimal balance of the two effects, but a GEOM term larger than that for the neutral complex has been produced.

As expected, the BSSE monotonically decreases (in absolute value) with the increasing basis set. The decrease is more rapid with the non-CP than with the CP optimization for the neutral complex. The BSSE seemingly does not depend strongly on the intermolecular geometric parameters of the complexes as may be concluded by comparing results from the 6-311++G** optimization and 6-311++G**//6-31G* single-point calculations. Whereas the O−H···O angle for the $CH_3OH\cdots OCB$ complex changes from 166.9° to 163.6° in the CP optimized structures calculated with the 6-31G* and the 6-311++G** basis sets, the BSSE of −1.50 kcal/mol changes only by 0.03 kcal/mol in the 6-311++G**//6-31G* single-point calculation. In the case of the 6-311++G**//6-31G* single-point calculation for the $CH_3NH_3^+\cdots OCB$ complex, BSSE changes even less, only by 0.01 kcal/mol, compared to the value obtained after 6-311++G** optimization, although the O···H separation differs considerably, by 0.038 Å from the 6-31G* and 6-311++G** optimizations.

The uncorrected binding energies increase (considering the negative sign) with the first three basis sets but then generally decrease slightly at the aug-cc-pvtz level. The BSSE corrected ΔE energies, ΔE^{cor}, show an even less general trend. The results indicate that the ΔE^{cor} values for the neutral complex differ by about 0.7 kcal/mol when the 6-31+G* and the aug-cc-pvtz basis sets were utilized in non-CP optimization, and the difference decreases to about 0.5 kcal/mol with the CP optimization. The 6-31+G* ΔE values are closer to the aug-cc-pvtz results than

TABLE 3: Structural Parameters and Binding Energy Terms for the $CH_3OH\cdots OCB$ and $CH_3NH_3^+\cdots OCB$ Complexes at the MP2 Level with Different Basis Sets[a]

	Non-CP Optimization					
	$CH_3OH\cdots OCB$		$CH_3NH_3^+\cdots OCB$			
	O···H	O−H···O	O···H	N−H···O	$N-H_{mon}$	$N-H_{comp}$
6-31G*	1.868	156.1	1.628	167.5	1.028	1.068
6-31+G*	1.842	168.4	1.648	172.6	1.028	1.063
6-311++G**	1.831	165.7	1.566	172.9	1.024	1.071
aug-cc-pvtz	1.819	161.3	1.570	172.7	1.022	1.069
	CP-Optimization					
	O···H	O−H···O	O···H	N−H···O		$N-H_{comp}$
6-31G*	1.939	166.9	1.663	170.9		1.064
6-31+G*	1.934	161.8	1.685	174.2		1.060
6-311++G**	1.935	163.6	1.625	174.9		1.063
aug-cc-pvtz	1.853	160.1	1.590	172.2		1.067

	$CH_3OH\cdots OCB$				$CH_3NH_3^+\cdots OCB$			
	non-CP		CP		non-CP		CP	
	BSSE	GEOM	BSSE	GEOM	BSSE	GEOM	BSSE	GEOM
6-31G*	−4.01	0.23	−2.83	0.11	−2.71	1.39	−2.54	1.10
6-31+G*	−2.62	0.17	−2.28	0.12	−2.43	1.09	−2.24	0.94
6-311++G**	−1.82	0.16	−1.50	0.11	−2.37	1.66	−2.00	1.21
6-311++G**// 6-31G*			−1.47	0.21			−1.99	1.24
aug-cc-pvtz	−0.94	0.21	−0.89	0.17	−1.12	1.61	−1.08	1.49
	ΔE^{uncor}	ΔE^{cor}	ΔE^{uncor}	ΔE^{cor}	ΔE^{uncor}	ΔE^{cor}	ΔE^{uncor}	ΔE^{cor}
6-31G*	−9.48	−5.47	−8.84	−6.01	−26.55	−23.83	−26.46	−23.93
6-31+G*	−8.80	−6.18	−8.64	−6.36	−25.81	−23.38	−25.72	−23.47
6-311++G**	−7.63	−5.81	−7.48	−5.98	−25.67	−23.30	−25.49	−23.49
6-311++G**// 6-31G*			−7.44	−5.97			−25.36	−23.37
aug-cc-pvtz	−7.80	−6.86	−7.77	−6.88	−25.58	−24.46	−25.55	−24.47

[a] Energies in kcal/mol, O···H distances in Å, O···H−X angles in deg. $\Delta E^{cor} = \Delta E^{uncor} - BSSE$.

those from 6-311++G** calculations (for the water dimer, the 6-31+G* ΔE values were closest to the Halkier et al. limit). For the $CH_3NH_3^+\cdots OCB$ complex, the 6-31+G* ΔE^{cor} values are less negative than the aug-cc-pvtz energies by 1.0−1.1 kcal/mol, which corresponds to an error of less than 5%. Overall, the present results suggest that the MP2/6-31+G* non-CP optimization provides O···H distances and ΔE^{cor} binding energies differing from the computationally much more demanding aug-cc-pvtz results by 0.02−0.08 Å and 0.7−1.1 kcal/mol.

The pragmatic "usefulness" of the application of a specific basis set may change for complexes of increasing number of heavy atoms. The calculated values support the use of the MP2/6-31+G* non-CP optimization and energy calculation for binding of larger cyclic ethers to amino acid side chain mimics. In the following section where 30 complexes are studied, the authors sought to answer whether this level of theory consistently reflects relative binding energies in compliance with fundamental chemical principles.

Other Complexes of Cyclic Ethers. Hydrogen-bonded complexes of cyclic ethers with different amino acid side chain mimics were compared from three points of view: (1) ring saturation, (2) ring size, and (3) the effects of the basis set and the optimization method on the structure and binding energy. The rings are comprised of four to six C and O atoms (Scheme 1), and there may be a double bond between atoms C_2 and C_3. Oxocyclobutene (OCBe), dihydrofuran (DHF), and oxocyclohexadiene-2,4 (OCHD) possess the $C_2{=}C_3$ double bond, whereas oxocyclobutane (OCB), tetrahydrofuran (THF), and oxocyclohexene-3 (OCHe) are saturated at this site.

Geometric Aspects. Structures optimized at the non-CP MP2/aug-cc-pvtz level are shown in Figures 1−5. The calculated intermolecular hydrogen-bond parameters as obtained from non-CP MP2/aug-cc-pvtz and MP2/6-31+G* geometry optimizations (first and second set, respectively), as well as from CP/MP2/6-31+G* geometry optimizations (third set), are summarized in Table 4. The O···H hydrogen-bond distances (where O is the ether oxygen and H belongs to the proton donor molecule) are considerably shorter when the bonds are formed with the saturated rings (considering OCHe as a member of this group as far as the saturated C_2-C_3 bond is concerned) as compared to hydrogen bonds with their unsaturated counterparts. The longer equilibrium O···H distances in complexes with OCBe, DHF, and OCHD have been attributed to the reduced basicity of the ether oxygen, which can come into existence by the conjugation of an oxygen lone pair with the π-electrons of the neighboring $C_\alpha{=}C_\beta$ double bond.

All amino acid mimics, except for the methyl-guanidium cation, can form only a single hydrogen bond to ethers. In the optimized methyl-guanidium complexes, the two $-NH_2$ groups form bifurcated hydrogen bonds between the $CH_3NHC(NH_2)_2^+$ cation and the ether oxygen for the most studied systems (Figure 5). For the $CH_3NHC(NH_2)_2^+\cdots OCHD$ pair, however, a single-hydrogen-bond structure was obtained upon the non-CP MP2/aug-cc-pvtz and MP2/6-31+G* geometry optimizations, making the hydrogen bond shorter than in the $CH_3NHC(NH_2)_2^+\cdots OCHe$ complex belonging to the "saturated" series.

Considering the effect of ring size on the intermolecular hydrogen-bond parameters for the OCB, THF, and OCHe as well as for the OCBe, DHF, and OCHD triads, the optimized

TABLE 4: Optimized Geometric Parameters for Hydrogen-Bonded Complexes of Cyclic Ethers with Amino Acid Mimics from ab Initio MP2 Calculations with or without CP-Optimization[a]

	OCB		THF		OCHe	
	O···H	O···H−X	O···H	O···H−X	O···H	O···H−X
CH_3OH	1.819	161.3	1.837	167.4	1.871	168.5
	1.842	168.4	1.871	164.5	1.884	167.6
	1.934	161.8	1.929	179.8	1.984	166.3
imidazole	1.822	163.9	1.805	166.0	1.853	170.5
	1.868	178.5	1.848	176.5	1.873	170.4
	1.948	180.0	1.933	178.4	1.961	167.6
$CH_3NH_3^+$	1.570	172.7	1.551	174.5	1.559	176.1
	1.648	172.6	1.632	175.4	1.637	177.2
	1.685	174.2	1.668	176.0	1.683	172.5
$imidazoleH^+$	1.563	175.9	1.542	178.4	1.563	174.8
	1.639	174.8	1.620	178.5	1.631	175.8
	1.682	176.5	1.662	179.7	1.679	174.8
CH_3GuaH^+	1.886	148.9	1.875	149.3	1.885	148.2
	1.913	147.7	1.902	147.9	1.917	147.3
	1.922	149.1	1.911	149.4	1.906	149.3
	1.940	148.4	1.934	148.5	1.940	147.4
	1.982	149.3	1.968	149.8	1.984	148.5
	1.998	148.7	1.992	148.8	1.985	148.3

	OCBe		DHF		OCHD	
	O···H	O···H−X	O···H	O···H−X	O···H	O···H−X
CH_3OH	1.915	157.5	1.887	169.0	1.969	164.3
	1.921	158.6	1.898	179.8	1.954	166.2
	2.025	157.5	2.010	177.2	2.029	163.9
imidazole	1.940	155.8	1.962	152.9	1.969	172.3
	1.920	175.4	1.955	153.7	1.955	170.2
	2.003	178.6	1.990	178.0	2.050	165.7
$CH_3NH_3^+$	1.631	172.7	1.611	174.8	1.670	174.8
	1.703	173.3	1.686	173.4	1.719	175.0
	1.740	174.9	1.726	174.1	1.766	174.0
$imidazoleH^+$	1.627	176.3	1.608	179.1	1.662	173.8
	1.696	176.7	1.677	179.2	1.710	175.9
	1.739	178.3	1.722	178.0	1.761	174.4
CH_3GuaH^+	1.935	148.4	1.924	148.7	1.825	163.0
	1.955	147.3	1.948	147.5		
	1.957	149.1	1.940	149.5	1.852	163.5
	1.989	147.6	1.983	147.4		
	2.020	149.1	2.015	149.2	2.015	149.9
	2.043	148.0	2.031	148.4	2.095	146.8

[a] O···H distances in Å, O···H−X angles in deg. X = O for CH_3OH and X = N in the other cases. Set 1−3 parameters are from non-CP MP2/aug-cc-pvtz, non-CP MP2/6-31+G*, and CP MP2/6-31+G* optimizations, respectively. The double sets for CH_3GuaH^+ are from non-CP MP2/aug-cc-pvtz, non-CP MP2/6-31+G*, and CP MP2/6-31+G* optimizations, respectively.

O···H separation has been found slightly changing without the indication of a clear trend. The CP optimization at the MP2/6-31+G* level leads to remarkable increase of the O···H distance compared to the non-CP procedure with neutral H-donor molecules (CH_3OH, imidazole), and, to a lesser extent, with protonated donors. The effect of the increased basis set in the non-CP geometry optimization, MP2/6-31+G* versus MP2/aug-cc-pvtz, is not unanimous regarding the O···H separation for the neutral complexes: the distance both decreases and increases by a few hundredths of an Å. In case of the ionic complexes, however, the O···H distance always shortens by 0.02−0.08 Å when the aug-cc-pvtz set is applied in the optimization.

The effects of the basis set and the optimization procedure on the O···H−X bond angle depend on the system in the case of the neutral complexes. Both effects are small, for instance, for the imidazole···OCHe and the CH_3OH···OCBe complexes. The basis set effect is large for the imidazole...OCBe complex (first- and second-row values), whereas the effect of the optimization method is remarkable for the imidazole···DHF system (second- and third-row values). No considerable effect of the two studied factors has been observed, however, for the O−H···X angle in the ionic species. The calculated range of the hydrogen-bond angle is 172−180° in complexes with $CH_3NH_3^+$ and the protonated imidazole. In bifurcated complexes with CH_3GuaH^+, the N−H···O angles are of 147−150°, and in the OCHD complex with a single hydrogen bond, the N−H···O angle is about 163°.

Energy Results. The BSSE and GEOM values are summarized in Table S1 (Supporting Information). The three sets of data were obtained after non-CP MP2/aug-cc-pvtz, non-CP MP2/6-31+G* optimizations and from MP2/6-311++G** single-point calculations at the CP/MP2/6-31G* optimized geometry.

The BSSE values clearly show dependence on the basis set, irrespective of the optimization method. As expected, the BSSE values decrease (in absolute value) when the basis set increases as 6-31+G*, 6-311++G**, and aug-cc-pvtz. Typical BSSE (absolute) values are of 2−4, 1−3, and 1−2 kcal/mol, respectively. Thus, the BSSE is fairly large even with the aug-cc-pvtz basis set: the values are of about 10−20% of the uncorrected binding energy for the neutral species and are of 5−10% of ΔE^{uncor} for the ionic species. The GEOM terms are small, 0.1−0.2 kcal/mol for the neutral species, independently of the optimization method and the basis set used for the calculation. The GEOM values are of 1−2 kcal/mol for the ionic species, and these values are also independent of the basis set applied. The uniformly increased GEOM values for the ionic complexes have been attributed to the stretched N−H bonds, which have been discussed above.

Uncorrected and BSSE corrected binding energies are summarized in Table 5. The calculated binding energies are clearly more negative by about 10−15 kcal/mol for the ionic species compared to the neutral complexes. The ΔE^{cor} values are always the most negative ones when calculated with the aug-cc-pvtz basis set, whereas the non-CP MP2/6-31+G* and MP2/6-311++G**//CP/MP2/6-31G* values are generally close to each other. For the neutral complexes, the aug-cc-pvtz ΔE^{cor} values are generally of 0.5−1.0 kcal/mol more negative than from the other calculations. The hydrogen bonds by the imidazole donor are stronger than that with methanol by about 1−2 kcal/mol at any considered level. Whereas the binding energies change only moderately with the increase of the ring size, the saturation of the $C_2{=}C_3$ bond has a clear effect on ΔE^{cor}: the corrected binding energies are 1−2 kcal/mol more negative in complexes where the indicated C−C bond is saturated. As mentioned above, the possible conjugation of an oxygen lone pair with the π electrons of the double bond reduces the basicity of the oxygen, leading to smaller stabilization upon the hydrogen-bond formation and resulting in an increase of the O···H distance as compared to the saturated analogue.

Qualitatively similar conclusions may be drawn from results for the ionic ether···amino acid mimic complexes. The ring size of the ether component only slightly affects the ΔE^{cor} value within a triad. ΔE^{cor} becomes, however, more negative by 3−5 kcal/mol going from the OCBe, DHF, and OCHD triad to the corresponding complexes with OCB, THF, and OCHe. Thus, for the ionic species, the reduced basicity for the acceptor component becomes more meaningful. The aug-cc-pvtz binding energies are 1−2 kcal/mol more negative than those calculated

TABLE 5: Uncorrected, ΔE^{uncor}, and BSSE Corrected Binding Energies, $\Delta E^{cor} = \Delta E^{uncor} - BSSE$, from ab Initio MP2 Calculations with or without CP-Optimization[a]

	OCB		THF		OCHe	
	ΔE^{uncor}	ΔE^{cor}	ΔE^{uncorr}	ΔE^{cor}	ΔE^{uncor}	ΔE^{cor}
CH_3OH	−7.80	−6.86	−7.60	−6.48	−8.00	−6.73
	−8.80	−6.18	−8.39	−5.39	−8.89	−5.42
	−7.44	−5.97	−7.80	−6.07	−7.55	−5.46
imidazole	−9.27	−7.97	−9.62	−8.19	−10.38	−8.70
	−10.05	−7.51	−10.31	−7.58	−10.78	−7.47
	−9.15	−7.40	−9.57	−7.67	−10.30	−7.62
$CH_3NH_3^+$	−25.58	−24.47	−26.11	−24.88	−24.72	−23.18
	−25.81	−23.38	−26.06	−23.62	−24.28	−20.99
	−25.36	−23.37	−25.93	−23.89	−24.13	−21.62
imidazoleH$^+$	−23.07	−21.70	−23.62	−22.12	−23.26	−21.23
	−23.72	−20.81	−24.10	−21.11	−23.14	−19.18
	−23.01	−20.69	−23.68	−21.22	−22.91	−19.40
CH_3GuaH^+	−22.76	−21.40	−23.13	−21.61	−22.15	−20.42
	−23.83	−20.50	−24.09	−20.54	−23.26	−19.16
	−22.48	−20.40	−23.08	−20.62	−22.06	−19.32
	OCBe		DHF		OCHD	
	ΔE^{uncor}	ΔE^{cor}	ΔE^{uncorr}	ΔE^{cor}	ΔE^{uncor}	ΔE^{cor}
CH_3OH	−5.99	−5.17	−5.87	−5.03	−6.25	−5.12
	−6.99	−4.64	−7.02	−4.54	−7.33	−4.11
	−5.86	−4.47	−6.02	−4.50	−6.17	−4.32
imidazole	−7.80	−6.58	−8.50	−7.02	−8.06	−6.58
	−8.22	−5.92	−8.86	−5.92	−8.89	−5.73
	−7.43	−5.86	−7.91	−6.01	−8.13	−5.77
$CH_3NH_3^+$	−20.81	−19.78	−21.02	−19.89	−21.28	−19.79
	−20.94	−18.81	−21.16	−18.71	−21.30	−18.09
	−20.39	−18.68	−20.74	−18.88	−20.90	−18.24
imidazoleH$^+$	−18.82	−17.54	−19.11	−17.72	−19.33	−17.52
	−19.39	−16.81	−19.75	−16.89	−19.85	−16.14
	−18.16	−16.11	−19.11	−16.82	−19.14	−16.04
CH_3GuaH^+	−19.01	−17.71	−19.07	−17.65	−19.41	−17.44
	−19.79	−16.84	−20.09	−16.73	−19.54	−15.51
	−18.37	−16.24	−19.10	−16.68	−18.72	−15.68

[a] Energies in kcal/mol. Sets 1 and 2 from MP2/aug-cc-pvtz and MP2/6-31+G* calculations, respectively, without CP-optimization. Set 3: MP2/6-311++G**//CP/MP2/6-31G* single-point values. The corresponding BSSE values are from Table S1.

with the 6-31+G* and the 6-311++G** basis sets. From data in the table, the $CH_3NH_3^+$···cyclic ether hydrogen bonds are more stable by about 2−3 kcal/mol than those where the protonated imidazole or the methylguanidium cation are the proton donor. In case of CH_3GuaH^+, even the possibility for the bifurcated hydrogen bond does not increase the binding energy.

As a partial summary, the results suggest that the O···H distances and the binding energies for the studied hydrogen-bonded complexes of cyclic ethers and amino acid mimics may be generally determined with an uncertainty of a few hundredths of an Å and of about 1 kcal/mol, respectively, by applying the non-CP MP2/6-31+G* as compared to MP2/aug-cc-pvtz geometry optimization for neutral systems. In cases of ionic species, the O···H separation is 0.03−0.08 Å larger and the corrected binding energy is 1−2 kcal/mol less negative with the smaller basis set (Tables 4 and 5).

For calculating the enthalpy instead of the energy of formation of the hydrogen-bonded complex, the change in the zero-point energy throughout the process, ΔZPE, is required. ΔZPE showed moderate basis set dependence for the water dimer (Table 2), and a reasonable estimate for this quantity was obtained even at the MP2/6-31G* value. Table S2 in the Supporting Information provides the calculated values for the 6 × 5 pairs calculated both from CP and non-CP optimizations at the MP2/6-31G* level as well as from non-CP MP2/6-31+G* optimizations. The ΔZPE values are in the energy ranges of 0.53−1.62 and 0.54−1.71 kcal/mol with CP and non-CP optimizations, respectively. The largest difference of up to 0.37 kcal/mol was calculated for the methanol complexes by using the two optimization methods. The CP versus non-CP optimization resulted in, however, only up to 0.1 kcal/mol differences in the ΔZPE for the ionic complexes. The ΔZPE values differ by no more than 0.2 kcal/mol when the MP2/6-31G* and the MP2/6-31+G* results are compared after non-CP optimization. Overall, these results indicate that the ΔZPE values are fairly stable as calculated with affordable basis sets.

Conclusions

Binding energies for hydrogen-bonded complexes of six cyclic ethers having four to six C and O ring atoms, with five hydrogen-bond donor molecules mimicking amino acid side chains, have been calculated at the MP2/6-31G*, MP2/6-31+G*, and MP2/aug-cc-pvtz levels, with and without counterpoise correction throughout the structure optimizations. Single-point calculations were performed at the MP2/6-311++G** level at the CP/MP2/6-31G* optimized geometries. The CP optimizations result in O···H equilibrium distances sometimes 0.1 Å longer than that obtained from non-CP optimizations. No such large deviations have been found for the O···H−X (X═O, N) angles. Despite the large geometric deviations calculated in cases with the two kinds of geometry optimization, the BSSE corrected binding energies are close to each other, as well as the changes in the zero-point energy throughout the hydrogen-bond formations. The basis set superposition error decreases with an increasing basis set but still amounts to 10−20% and 5−10% of the uncorrected binding energy for the neutral and ionic ether complexes, respectively, at the MP2/aug-cc-pvtz level. The geometry distortion energy for the elements upon hydrogen-bond formation amounts to a few tenths of a kcal/mol for neutral complexes. This term is 1−2 kcal/mol for protonated systems, where the N−H distance involved in the hydrogen-bond stretches by about 0.04 Å as compared to its optimized value in the isolated molecule. The remarkable bond stretching upon hydrogen-bond formation is independent of the applied basis set.

The ring size has proven to exert a minor effect on the calculated binding energy. In contrast, the binding energies for the studied complexes having a single bond in the ether component at the $C_\alpha-C_\beta$ position are more negative by 1−2 and 3−5 kcal/mol for the neutral and the ionic species, respectively, than those for the counterparts with a C═C double bond next to ring oxygen. The less negative hydrogen-bond formation energy, as well as the increased O···H separation in the latter case, has been attributed to the reduced basicity of the ether oxygen, which can come into existence by the conjugation of an oxygen lone pair with the π-electrons of the neighboring $C_\alpha=C_\beta$ double bond.

The authors conclude that the hydrogen-bond distances and binding energies may be determined with uncertainties of a few hundredths of an Å and of about 1 kcal/mol in comparison with the MP2/aug-cc-pvtz values for neutral ether complexes at a reasonable computational cost by performing non-CP optimization at the MP2/6-31+G* level. The foreseeable overestimation of the O..H distance at this level is 0.03−0.08 Å for ionic species, whereas the binding energy may be calculated less negative by 1−2 kcal/mol with the smaller basis set. These fairly

good results are considered as fortuitous error cancellation because of the basis set insaturation and the calculated BSSE. Further studies are thus needed to determine whether the MP2/6-31+G* level of theory would provide results with deviations within the above limit from the high-level MP2/aug-cc-pvtz values for other classes of hydrogen-bonded complexes as well. The present study is the first step toward the development of an affordable computational level for estimating the binding energies of natural products having fused ring ether substructures to various receptor systems such as the human estrogen receptors.

Acknowledgment. The authors are thankful to Drs. Alagona and Ghio for the valuable discussions. P. Nagy thanks the Ohio Suprecomputer Center for the granted computer time and the technical support by Dr. Brozell. The USDA grant support provided to P. Erhardt is also acknowledged.

Supporting Information Available: The BSSE and GEOM values and the calculated zero-point energy values for the 6 × 5 pairs calculated from both CP and non-CP optimizations at the MP2/6-31G* level as well as from non-CP MP2/6-31+G* optimizations. This material is available free of charge via the Internet at http://pubs.acs.org.

References and Notes

(1) See, for example, (a) *Activation and Functionalization of C-H Bonds*; Goldberg, K. I., Goldman, A. S., Eds.; ACS Symposium Series 885; American Chemical Society: Washington, DC, 2004. (b) Barnes, A. J.; Limbach, H.-H. *J. Mol. Struct.* **2004**, *700* (1−3), 1. (c) Desiraju, G.; Steiner, T. *The Weak Hydrogen Bond: Applications to Structural Chemistry and Biology;* Oxford University Press: New York, 1999. (d) Scheiner, S. *Hydrogen Bonding: A Theoretical Perspective*, Oxford University Press: New York, 1997. (e) *An Introduction to Hydrogen Bonding*; Jeffrey, G. A., Ed.; Oxford University Press: New York, 1997. (f) *Modeling the Hydrogen Bond*; Smith, D. A., Ed.; ACS Symposium Series 569; American Chemical Society: Washington, DC, 1994.

(2) (a) The Chemistry of Functional Groups, Suppl. E. In *The Chemistry of Ethers, Crown Ethers, Hydroxyl Groups and Their Sulfur Analogs;* Patai, S., Ed.; John Wiley and Sons: Chichester, U.K., 1980; Parts 1 and 2. (b) Rodd's Chemistry of Carbon Compounds. In *Monohydric Alcohols, Their Ethers and Esters, Sulphur Analogues, Nitrogen Derivatives, Organometallic Compounds;* Coffey, S., Ed.; Elsevier: New York, 1965; Vol. 1B.

(3) (a) Buehl, M.; Ludwig, R.; Schurhammer, R.; Wipff, G. *J. Phys. Chem. A* **2004**, *108*, 11463. (b) Stoyanov, E. S.; Reed, C. A. *J. Phys. Chem. A* **2004**, *108*, 907. (c) Buehl, M.; Wipff, G. *J. Am. Chem. Soc.* **2002**, *124*, 4473. (d) Grootenhuis, P. D.; Kollman, P. A. *J. Am. Chem. Soc.* **1989**, *111*, 4046. (e) Zeng, X.; Yang, X. *J. Phys. Chem. B* **2004**, *108*, 17384. (f) Dimitrova, Y.; Tsenov, J. *THEOCHEM* **2004**, *683*, 65. (g) Wierzejewska, M.; Saldyka, M. *Chem. Phys. Lett.* **2004**, *391*, 143. (h) Herrebout, W. A.; Delanoye, S. N.; van der Veken, B. J. *J. Phys. Chem. A* **2004**, *108*, 6059. (i) Han, S. W.; Kim, K. *J. Mol. Struct.* **1999**, *475*, 43. (j) Chowdhury, P. K. *J. Phys. Chem. A* **2000**, *104*, 7233. (k) Macleod, N. A.; Simons, J. P. *Chem. Phys.* **2002**, *283*, 221.

(4) (a) Doerksen, R. J.; Chen, B.; Liu, D.; Tew, G. N.; DeGrado, W. F.; Klein, M. L. *Chem.*—Eur. J. **2004**, *10*, 5008. (b) Gil, F. P. S. C.; Teixeira-Dias, J. J. C. *J. Mol. Struct.* **1999**, *482*, 621. (c) Marstokk, K.-M.; Moellendal, H. *Acta Chem. Scand.* **1995**, *49*, 728. (d) Simon, J. P.; Eriksson, K.-E. L. *J. Mol. Struct.* **1996**, *384*, 1.

(5) Keasling, H.; Schueler, F. *J. Am. Pharm. Assoc.* **1950**, *39*, 87.

(6) Kavlock, R. J.; Daston, G. P.; DeRosa, C.; Fenner-Crisp, P.; Gray, L. E.; Kaattari, S.; Lucier, G.; Luster, M.; Mac, M. J.; Maczka, C.; Miller, R.; Moore, J.; Rolland, R.; Scott, G.; Sheehan, D. M.; Sinks, T.; Tilson, H. A. *Environ. Health Perspect.* **1996**, *104* (Suppl. 4), 715.

(7) Hehre, W. J.; Radom, L.; Schleyer, P. v. R.; Pople, J. A. *Ab Initio Molecular Orbital Theory*; Wiley: New York, 1986.

(8) (a) Møller, C.; Plesset, M. S. *Phys. Rev.* **1934**, *46*, 618. (b) Pople, J. A.; Binkley, J. S.; Seeger, R. *Int. J. Quantum Chem.* **1976**, *10s*, 1. (c) Krishnan, R.; Frisch, M. J.; Pople, J. A. *J. Chem. Phys.* **1980**, *72*, 4244. (d) Pople, J. A.; Head-Gordon, M.; Raghavachari, K. *J. Chem. Phys.* **1987**, *87*, 5968.

(9) (a) Kendall, R. A.; Dunning, T. H., Jr.; Harrison, R. J. *J. Chem. Phys.* **1992**, *96*, 6796. (b) Woon, D. E.; Dunning, T. H., Jr. *J. Chem. Phys.* **1994**, *100*, 2975.

(10) McQuarrie, D. A. *Statistical Mechanics*; University Science Books: Sausalito, CA, 2000.

(11) (a) Sokalski, W. A.; Roszak, S.; Hariharan, P. C.; Kaufman, J. J. *Int. J. Quantum Chem.* **1983**, *23*, 847. (b) van Duijneveldt, F. B.; van Duijneveldt-van de Rijdt, J. G. C. M.; van Lenthe, J. H. *Chem. Rev.* **1994**, *94*, 1873.

(12) Boys, S. F.; Bernardi, F. *Mol. Phys.* **1970**, *19*, 553.

(13) Smit, P. H.; Derissen, J. L.; van Duijneveldt, F. B. *J. Chem. Phys.* **1978**, *69*, 4241.

(14) Simon, S.; Duran, M.; Dannenberg, J. J. *J. Chem. Phys.* **1996**, *105*, 11024.

(15) Nagy, P. I.; Smith, D. A.; Alagona, G.; Ghio, C. *J. Phys. Chem.* **1994**, *98*, 486.

(16) Frisch, M. J.; Trucks, G. W.; Schlegel, H. B.; Scuseria, G. E.; Robb, M. A.; Cheeseman, J. R.; Montgomery, J. A., Jr.; Vreven, T.; Kudin, K. N.; Burant, J. C.; Millam, J. M.; Iyengar, S. S.; Tomasi, J.; Barone, V.; Mennucci, B.; Cossi, M.; Scalmani, G.; Rega, N.; Petersson, G. A.; Nakatsuji, H.; Hada, M.; Ehara, M.; Toyota, K.; Fukuda, R.; Hasegawa, J.; Ishida, M.; Nakajima, T.; Honda, Y.; Kitao, O.; Nakai, H.; Klene, M.; Li, X.; Knox, J. E.; Hratchian, H. P.; Cross, J. B.; Bakken, V.; Adamo, C.; Jaramillo, J.; Gomperts, R.; Stratmann, R. E.; Yazyev, O.; Austin, A. J.; Cammi, R.; Pomelli, C.; Ochterski, J. W.; Ayala, P. Y.; Morokuma, K.; Voth, G. A.; Salvador, P.; Dannenberg, J. J.; Zakrzewski, V. G.; Dapprich, S.; Daniels, A. D.; Strain, M. C.; Farkas, O.; Malick, D. K.; Rabuck, A. D.; Raghavachari, K.; Foresman, J. B.; Ortiz, J. V.; Cui, Q.; Baboul, A. G.; Clifford, S.; Cioslowski, J.; Stefanov, B. B.; Liu, G.; Liashenko, A.; Piskorz, P.; Komaromi, I.; Martin, R. L.; Fox, D. J.; Keith, T.; Al-Laham, M. A.; Peng, C. Y.; Nanayakkara, A.; Challacombe, M.; Gill, P. M. W.; Johnson, B.; Chen, W.; Wong, M. W.; Gonzalez, C.; Pople, J. A. *Gaussian 03*, revision C.02; Gaussian, Inc.: Wallingford, CT, 2004.

(17) Hobza, P.; Havlas, Z. *Theor. Chem. Acc.* **1998**, *99*, 372.

(18) Halkier, A.; Koch, H.; Jorgensen, P.; Christiansen, O.; Beck Nielsen, I. M.; Helgaker, T. *Theor. Chem. Acc.* **1997**, *97*, 150.

(19) Odutola, J. A.; Dyke, T. R. *J. Chem. Phys.* **1980**, *72*, 5062.

(20) Curtiss, L. A.; Fruip, D. J.; Blander, M. *J. Chem. Phys.* **1979**, *71*, 2703.